

Conformational analysis and interpretation of $\nu(\text{OH})$ bands in the IR spectra of 1'-hydroxyethyl derivatives of 1,4-benzo- and 5,8-dihydroxy-1,4-naphthoquinones: a DFT study

V. P. Glazunov,* D. V. Berdyshev, N. D. Pokhilo, and V. F. Anufriev

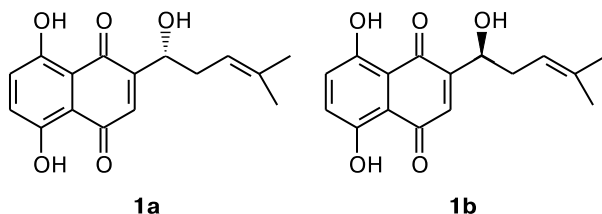
Pacific Institute of Bioorganic Chemistry, Far-Eastern Branch of the Russian Academy of Sciences,
159 prosp. 100 let Vladivostoku, 690022 Vladivostok, Russian Federation.

Fax: +7 (423 2) 31 4050. E-mail: glazunov@piboc.dvo.ru

Detailed conformational analysis of the molecule of 1'-hydroxyethyl-1,4-benzoquinone (**3**) by the B3LYP/cc-pVTZ method revealed predominance of rotamers with the free 1'-OH group in the gas phase. B3LYP/cc-pVTZ calculations with inclusion of solvent (cyclohexane) effect in the framework of the polarizable continuum model predict an increase in the percentage of such rotamers compared to the corresponding gas-phase values. The results obtained are in qualitative agreement with the experimentally observed pattern of $\nu(\text{OH})$ bands in the IR spectrum of compound **3** in cyclohexane (hexane) solution. Conformational analysis, including tautomerism and rotamerism, of 2-ethyl-1',5,8-trihydroxy-1,4-naphthoquinone (**2**) was performed by the B3LYP method with the 6-31G(d), 6-311G(d), 6-311G(d,p), and cc-pVDZ basis sets. The most abundant tautomeric form of compound **2** is form **A** in which the substituent bearing 1'-OH group is in the quinonoid nucleus. In the gas phase, the percentage of all rotamers in form **A** is about 86% (among them, the proportion of rotamers with the free 1'-OH group is more than 60%). The main reason for splitting of the $\nu(\text{OH})$ bands in the IR spectra of compounds **2** and **3** in solutions in nonpolar solvents is the equilibrium between rotamers with a relatively weak intramolecular hydrogen bond between the 1'-OH group and the carbonyl group and those having no this bond.

Key words: 1'-hydroxyethyl-1,4-benzoquinone; 2-ethyl-1',5,8-trihydroxy-1,4-naphthoquinone, 2-ethyl-1'-hydroxynaphthazarin, quantum chemical calculations, density functional theory, potential energy surface; conformational analysis; rotamerism, tautomerism; IR spectroscopy.

In ancient times, extracts from roots of *Alkanna tinctoria* in Europe and from *Lithospermum erithrorhizon* in Eastern countries were used as natural dark-red dyes. In the early 20th century, enantiomeric naphthoquinones shikonin (**1a**) and alkannin (**1b**) (racemic mixture of **1a** and **1b** is called shikalkin) were isolated¹ from extracts of roots of these plants and identified.²



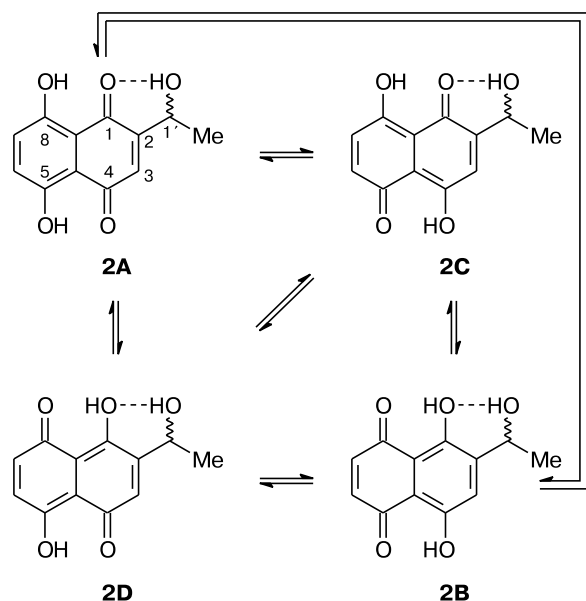
More recently,^{3,4} these natural substances have been found in many plants of the *Boraginaceae* family in the form of free alcohols and their esters. They exhibit a variety of interesting biological properties including antibac-

terial,⁵ antifungal,⁶ anti-inflammatory,^{7,8} anticancer,⁹ analgesic,^{7,10} and antipyretic ones,¹¹ as well as immunostimulating activity.¹²

Tautomerism in 1'-hydroxyalkylnaphthazarines is still a moot question. Numerous attempts to reveal prototropic tautomerism in, e.g., shikalkin in solutions by ¹H and ¹³C NMR spectroscopy have been made earlier.^{13–15} However, the determination of the tautomeric composition of shikalkin in solutions failed owing to high rate of tautomeric transitions in naphthazarines (on the time scale of NMR spectroscopy). Moreover, three different conclusions have been made about the tautomeric form (Scheme 1) in which this compound exists in solution, viz., only forms **C** and **D** (see Ref. 13), all forms **A–D** (see Ref. 14), or mainly form **A** (see Ref. 15).

Recently,¹⁶ we have studied prototropic tautomerism in 1'-hydroxyalkylnaphthazarines in solutions in nonpolar solvents (CCl₄, *n*-hexane or cyclohexane) by IR spectroscopy taking ethyl-1',5,8-trihydroxy-1,4-naphthoquinone (1'-hydroxyethylnaphthazarine (**2**)) as an example. It was

Scheme 1



assumed that intramolecular hydrogen bonds (IMHB) $O(1')-H...O(1)^*$ in the "quinonoid" (**2A**) and "benzenoid" (**2B**) tautomers have different stability. Because of this, the frequencies of the $\nu(\text{OH})$ absorption bands of tautomers **2A** and **2B** in the IR spectra of compound **2** should be significantly different. This would help to follow the changes in the tautomeric composition of compound **2** in solutions. Indeed, the IR spectrum of a solution of compound **2** in CCl_4 exhibits two high-frequency $\nu(\text{OH})$ bands whose frequencies differ by 50 cm^{-1} . This can be explained by the assumed tautomeric equilibrium $2A \rightleftharpoons 2B$. However, in the spectrum of compound **2** in hexane (cyclohexane) solution the low-frequency band, which is tentatively assigned to the quinonoid tautomer **2A**, is split into three strongly overlapped components (Fig. 1). Emphasize that hexane (cyclohexane) is a solution of lower polarity than CCl_4 . Decomposition of the contour of the low-frequency $\nu(\text{OH})$ band gave three frequencies, namely, 3570 , 3589 , and 3605 cm^{-1} . Thus, the peak-to-peak separations are 19 and 16 cm^{-1} . For the components at 3589 and 3570 cm^{-1} the areas-under-curve are nearly the same, whereas the area-under-curve for the component at 3605 cm^{-1} is 2.3 times smaller. In the spectrum of a solution of compound **2** in hexane, the high-frequency $\nu(\text{OH})$ band at 3635 cm^{-1} has an asymmetric contour. Its approximation by Lorentzian and Gaussian functions revealed contributions from at least two components. A possible reason is that not only tautomers **2A** and **2B**, but also the "1,5-quinonoid" tautomer **2C** and the "4,8-quinonoid" tautomer **2D** are present in solution.¹⁶

* Figures in parentheses denote the number of the carbon atom bearing the oxygen atom.

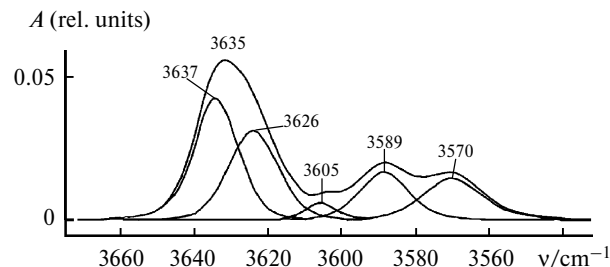


Fig. 1. IR spectra of a solution of compound **2** in hexane.

Analysis of the contour of the $\nu(\text{OH})$ absorption band in the spectrum of compound **2** in CCl_4 solution showed that, formally (due to broadening of spectral components), the observed splitting into two components is about 50 cm^{-1} . This indicates that the $1'-\text{OH}$ group participates in the formation of very weak IMHB. The maximum of the high-frequency component of the $\nu(\text{OH})$ band in the IR spectrum of a solution of **2** in hexane (cyclohexane) is at 3635 cm^{-1} , which is close to the $\nu(\text{OH})$ frequency in aliphatic alcohols. Based on the splitting $\Delta\nu$, the IMHB in compound **2** is comparable with IMHB in the *o*-vinylphenol molecule;^{17,18} in the spectrum of the latter the band corresponding to the free OH group is much stronger than the band corresponding to the bound OH group. An explanation for this phenomenon is as follows¹⁸: the proportion of the rotamers with IMHB determined with inclusion of the solvent (CCl_4) effect is at most 24%.

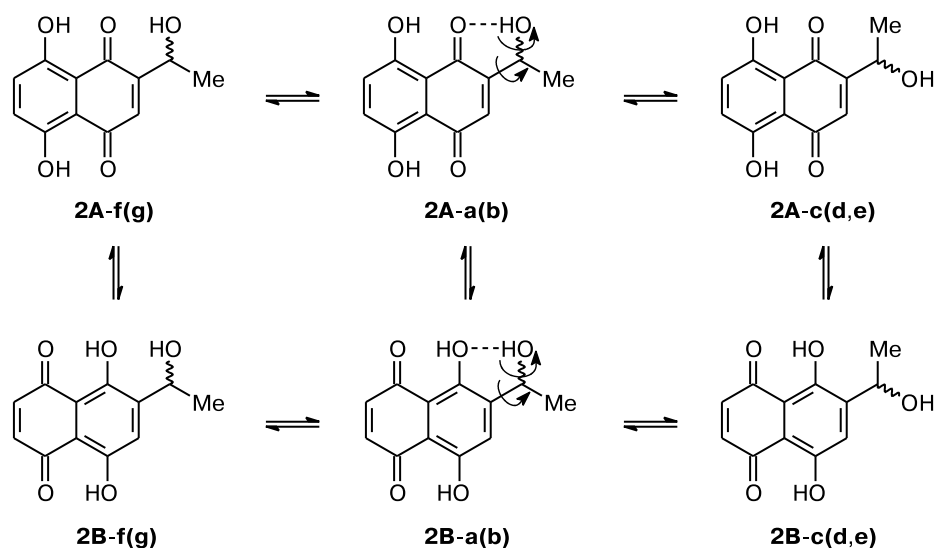
One can assume that, in addition to prototropic tautomerism, the following equilibria are also possible for compound **2** in solutions in nonpolar solvents: $2A-a(b) \rightleftharpoons 2A-f(g)$, $2A-a(b) \rightleftharpoons 2A-c(d,e)$, $2B-a(b) \rightleftharpoons 2B-f(g)$, and $2B-a(b) \rightleftharpoons 2B-(d,e)$. These equilibria are accompanied by cleavage of the IMHB involving the $1'-\text{OH}$ group (Scheme 2 and Figs 2 and 3).

To establish the reasons for the complex pattern of the $\nu(\text{OH})$ bands in the spectra of compound **2**, we synthesized $1'-\text{hydroxyethyl-1,4-benzoquinone}$ (**3**) (Scheme 3), which possesses no prototropic tautomerism. Molecule **3** represents a model for the quinonoid fragment of molecule **2** in the tautomeric form **A**. To study the effect of tautomerism and rotamerism in the $1'-\text{hydroxyalkyl}$ substituent on the spectral characteristics of compounds **2** and **3**, we performed conformational analysis of these molecules with the B3LYP density functional in different basis sets.

Results and Discussion

The IR spectra of solutions of compounds **2** and **3** in CCl_4 exhibit high-frequency $\nu(\text{OH})$ doublets with a splitting of about 50 cm^{-1} . Owing to the narrowing of spectral bands, the spectrum of a solution of compound **3** in hexane (cyclohexane) clearly exhibits a splitting of the low-frequency $\nu(\text{OH})$ band into two components with a peak-to-peak separation of nearly 16 cm^{-1} . The high-frequency

Scheme 2



band at 3635 cm^{-1} has a slightly asymmetric contour (Fig. 4); its decomposition using Lorentzian and Gaussian functions reveals contributions from at least two com-

ponents. The IR spectra of solutions of compounds **2** and **3** in hexane match each other, except for a weak band at 3605 cm^{-1} , which is observed for **2** only.

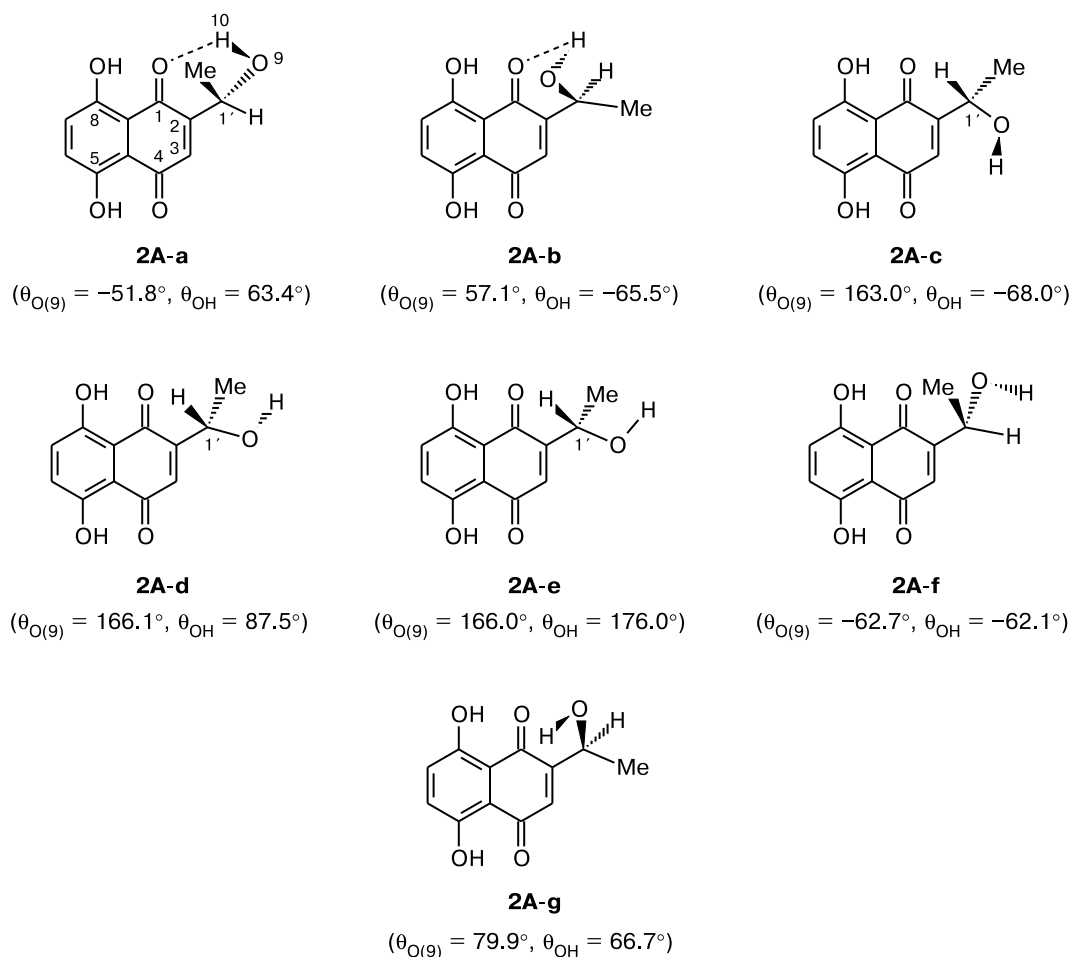


Fig. 2. Structures of rotamers of the quinonoid tautomers **2A**.

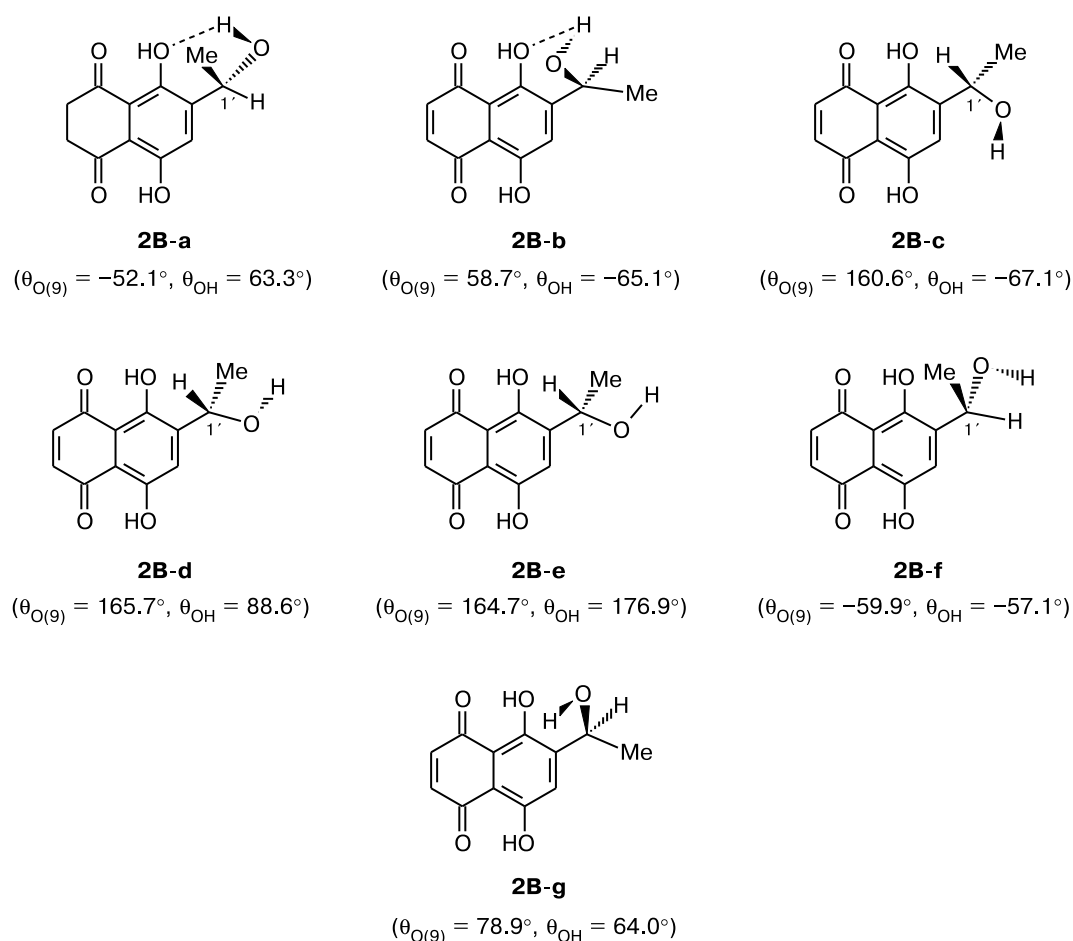
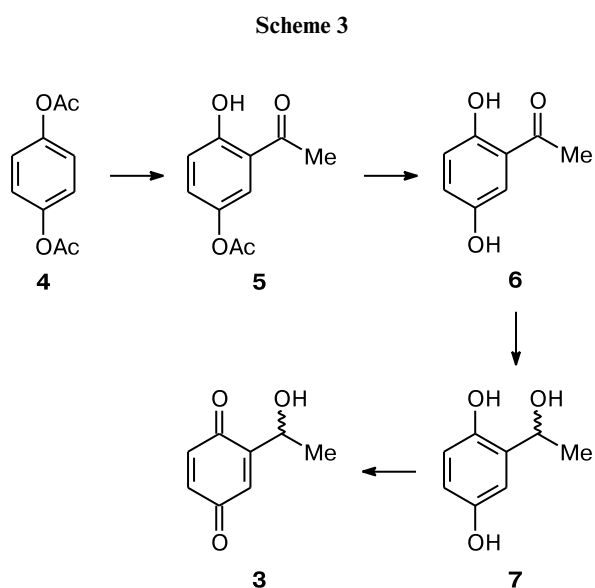
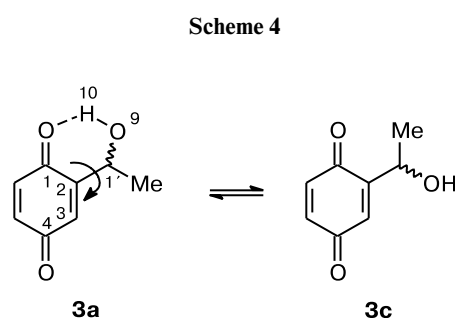


Fig. 3. Structures of rotamers of the benzenoid tautomers **2B**.



Analysis of the spectrum of a solution of the structurally simpler compound **3** in hexane shows that the contour of the $\nu(\text{OH})$ absorption band of the $1'$ -OH group is

a superposition of at least four components. The larger splitting of about $54\text{--}55\text{ cm}^{-1}$ between the maximum of the band at 3635 cm^{-1} and the center of gravity of the two components at 3586 and 3570 cm^{-1} can be attributed to rotamers **3a** and **3c** present in solution (Scheme 4). The nature of the smaller splitting of about 16 cm^{-1} ($3586\text{--}3570\text{ cm}^{-1}$) is still unclear.



To locate all possible isomers of compound **3**, we used the B3LYP/6-31G method to construct a two-dimensional (2D) section of the potential energy surface (PES, $E_0(\vec{R})$)

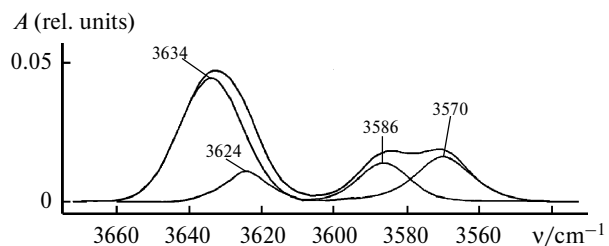


Fig. 4. IR spectrum of a solution of compound **3** in hexane.

of system **3** in the plane of the torsion angles $\theta_{O(9)}$ ($O(9)-C(1')-C(2)-C(1)$) and θ_{OH} ($H(10)-O(9)-C(1')-C(2)$) (from this point on, "the 2D cyclic potential" $v(\theta_{O(9)}, \theta_{OH})$). When using high-level quantum chemical methods and extended basis sets, this procedure permits correct identification of the regions in the configuration space corresponding to the potential wells and saddle points on the PES. In the case of compound **3** it is sufficient to use the density functional theory (DFT) with hybrid exchange-correlation functionals (e.g., B3LYP) and the split-valence AO basis sets of 6-31G quality (and more extended basis sets). The applicability of the B3LYP method to solving such problems has been demonstrated earlier.^{18–23}

Assuming that the first step of conformational analysis involves only the establishment of possible conformations of isomers of the compound under study and no exact determination of their relative energies and geometric parameters, the requirements for the quantum chemical method to be used can be not too stringent. For instance, in a study of the conformational mobility of *o*-vinylphenol we have shown^{18,24} that the 2D sections of the PES obtained from the AM1, MP2/6-31G, and B3LYP/6-311G(d) calculations are qualitatively similar and correctly reproduce details of the dynamic behavior of the molecular system.

Figure 5 presents the 2D cyclic potential $V(\theta_{O(9)}, \theta_{OH})$ obtained from B3LYP/6-31G calculations of compound **3**. Scanning was performed on a uniform grid with an increment of -5.0° for each coordinate. For clarity, possible pathways of transitions between rotamers are shown in Fig. 5 where the coordinates were varied from 165° to -295° ($\theta_{O(9)}$) and from 80° to -355° (θ_{OH}).

Analysis of the PES thus constructed showed that compound **3** has seven rotamers **3a–g**. The PES shown in Fig. 5 demonstrates only six out of seven minima because the potential well for rotamer **3g** (about $0.36 \text{ kcal mol}^{-1}$) is very shallow at this scale (neighboring isolines are separated by $0.8 \text{ kcal mol}^{-1}$). The minimum corresponding to rotamer **3g** is shown by the dashed line.

Full geometry optimization of rotamers **3a–e** was carried out by the B3LYP method in the 6-311G(d), 6-311G(d,p), cc-pVDZ, and cc-pVTZ basis sets. The geometry of rotamers **3f,g** was optimized only in the

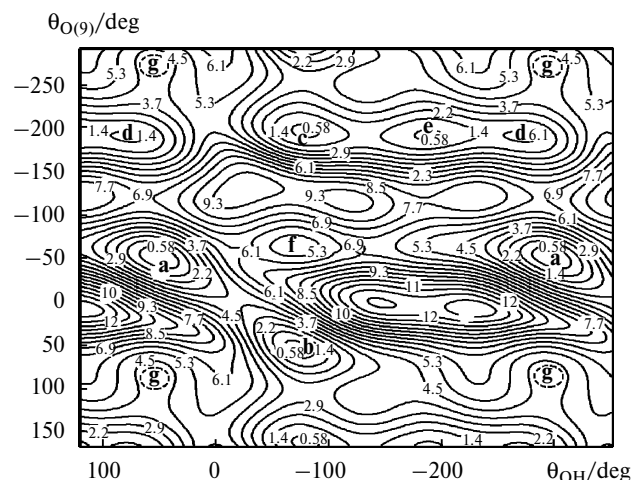
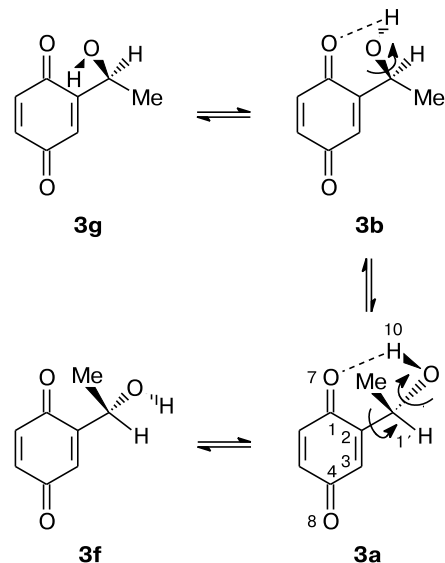


Fig. 5. 2D cyclic PES of compound **3**.

6-311G(d) basis set, because their percentage is negligible and they were left out of consideration (see below). Only in two rotamers (**3a,b**) the 1'-OH group is involved in the formation of IMHB with the O atom of the C(1)O carbonyl group (Scheme 5). The global minimum on the PES ($E_0(R^{\rightarrow})$) corresponds to rotamer **3a** (Table 1). The relative energy of rotamer **3b** calculated in the cc-pVTZ basis set is $0.11 \text{ kcal mol}^{-1}$.* The geometric parameters of rotamers **3a** and **3b** are as follows: $R(O(7)-O(9)) = 2.826$ and 2.820 \AA , $R(H(10)-O(7)) = 2.118$ and 2.820 \AA , the angle $O(7)-H(10)-O(9) = 128.9^\circ$ and 128.4° , $\theta_{OH} = 62.24^\circ$ and -64.18° . Among these parameters, the θ_{OH} angles differ to the greatest extent.

Scheme 5



* From this point on, by default we will discuss the energy and geometric characteristics calculated in the cc-pVTZ basis set.

Table 1. Electronic energies (E_0 /au), total energies ($(E = E_0 + \text{ZPE})$ /au), the Gibbs free energies (G /au), enthalpies (ΔH /kcal mol $^{-1}$), relative Gibbs free energies (ΔG /kcal mol $^{-1}$), percentages ($g^{\%}$ (%)), $\nu(\text{OH})$ frequencies/cm $^{-1}$, and intensities A (rel. units) calculated for rotamers of 1'-hydroxyethylbenzoquinone **3**

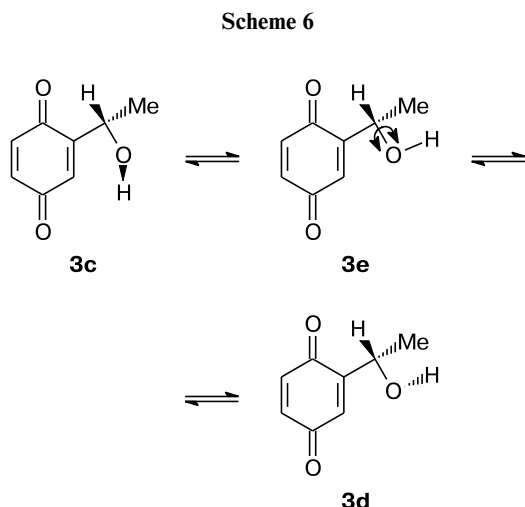
Rotamer	Computational method	$-E_0$	$-E$	$-G$	$-H$	ΔG	$g^{\%}$	ν/A
3a	B3LYP/6-311G(d)	535.428663	535.282242	535.317671	35.271317	0.23	22.99	3736.8/1.00
	B3LYP/6-311G(d) ^a	535.441124	535.294834	535.330374	535.283877	0.38	19.86	3733.3/1.00
	B3LYP/6-311G(d,p)	535.445472	535.299351	535.334807	535.288410	0.25	22.86	3767.3/1.00
	B3LYP/cc-pVDZ	535.334981	535.188997	535.224388	535.178096	0.13	26.62	3701.7/1.00
	B3LYP/cc-pVTZ	535.500178	535.353975	535.389470	535.343029	0.20	21.67	3751.5/1.00
	B3LYP/cc-pVTZ ^b	535.500178	535.361286	535.397157	535.349925	0.19	21.79	3564
	B3LYP/cc-pVTZ ^a	535.513188	535.366898	535.402438	535.310953	0.41	18.13	—
3b	B3LYP/6-311G(d)	535.428506	535.281942	535.317316	535.271098	0.46	15.78	3748.4/1.19
	B3LYP/6-311G(d) ^a	535.440862	535.294497	535.329887	535.283628	0.68	11.86	3741.4/1.13
	B3LYP/6-311G(d,p)	535.444950	535.298747	535.334175	535.287872	0.65	11.71	3777.2/1.19
	B3LYP/cc-pVDZ	535.334264	535.188179	535.223510	535.177356	0.68	10.52	3709.4/1.21
	B3LYP/cc-pVTZ	535.500003	535.353686	535.389161	535.342802	0.39	15.62	3765.0/1.10
	B3LYP/cc-pVTZ ^b	535.500003	535.361002	535.396851	535.349709	0.38	15.76	3577
	B3LYP/cc-pVTZ ^a	535.512956	535.366392	535.401981	535.355548	0.69	11.18	—
3c	B3LYP/6-311G(d)	535.428277	535.282298	535.318043	535.271168	0.00	34.09	3775.0/0.35
	B3LYP/6-311G(d) ^a	535.441027	535.295187	535.330976	535.284038	0.00	37.58	3773.7/0.46
	B3LYP/6-311G(d,p)	535.445149	535.299453	535.335206	535.288308	0.00	34.89	3821.3/0.47
	B3LYP/cc-pVDZ	535.334578	535.188952	535.224600	535.177859	0.00	33.15	3767.5/0.35
	B3LYP/cc-pVTZ	535.499843	535.354010	535.389781	535.342860	0.00	30.12	3811.2/0.51
	B3LYP/cc-pVTZ ^b	535.499843	535.361302	535.397462	535.349738	0.00	30.09	3621
	B3LYP/cc-pVTZ ^a	535.515135	535.369156	535.403084	535.358026	0.00	35.94	—
3d	B3LYP/6-311G(d)	535.426865	535.280928	535.316631	535.269794	0.89	7.64	3766.4/0.38
	B3LYP/6-311G(d) ^a	535.439773	-535.293741	535.329403	535.282666	0.99	7.10	3766.4/0.61
	B3LYP/6-311G(d,p)	535.444061	535.298333	535.334009	535.237216	0.75	9.82	3813.9/0.45
	B3LYP/cc-pVDZ	535.333649	535.188047	535.223665	535.176966	0.59	12.25	3756.8/0.34
	B3LYP/cc-pVTZ	535.498773	535.353047	535.388801	535.341871	0.61	10.67	3805.1/0.48
	B3LYP/cc-pVTZ ^b	535.498773	535.360333	535.396477	535.348742	0.62	10.60	3615
	B3LYP/cc-pVTZ ^a	535.512136	535.366199	535.401763	535.157071	0.83	8.90	—
3e	B3LYP/6-311G(d)	535.427703	535.281841	535.317516	535.270689	0.33	19.51	3800.9/0.48
	B3LYP/6-311G(d) ^a	535.440330	535.294678	535.330537	535.283458	0.28	23.60	3798.9/0.63
	B3LYP/6-311G(d,p)	535.444566	535.298997	535.334714	535.237813	0.31	20.72	3844.8/0.61
	B3LYP/cc-pVDZ	535.333873	535.188376	535.223989	535.177242	0.38	17.46	3790.6/0.46
	B3LYP/cc-pVTZ	535.499363	535.353695	535.389481	535.342486	0.19	21.92	3830.3/0.62
	B3LYP/cc-pVTZ ^b	535.499363	535.360978	535.397156	535.349356	0.19	21.76	3639
	B3LYP/cc-pVTZ ^a	535.512566	535.366704	535.402773	535.355552	0.20	25.85	—
3f	B3LYP/6-31G(d)	535.289596	535.143122	535.178953	535.131943	3.92	0.06	3735.8/0.22
	B3LYP/6-311G(d)	535.422032	535.276177	535.312032	535.264984	3.77	0.06	3774.0/0.30
3g	B3LYP/6-31G(d)	535.290340	535.143688	535.179702	535.132541	3.45	0.13	3717.3/0.17
	B3LYP/6-311G(d)	535.422654	535.276627	535.312672	535.265456	3.37	0.12	3755.3/0.23

^a Calculated with inclusion of solvent (cyclohexane) effect in the framework of the PCM model.^b Frequency calculations were carried out with a scale factor of 0.95.

Out of five rotamers with free 1'-OH group, two (**3f** and **3g**) are energetically most unfavorable; their relative energies (ΔE_0) calculated in the 6-311G(d) basis set are 4.16 and 3.77 kcal mol $^{-1}$, respectively. Rotamers **3c–e** (Scheme 6) have the following relative energies: $\Delta E_0(\mathbf{3c}) = 0.21$, $\Delta E_0(\mathbf{3d}) = 0.88$, and $\Delta E_0(\mathbf{3e}) = 0.51$ kcal mol $^{-1}$.

In the region $-310^\circ \leq \theta_{\text{O}(9)} \leq -235^\circ$ of the configuration space, the potential $V(\theta_{\text{O}(9)}, \theta_{\text{OH}})$ has a complex shape. This is due to steric factor (passage of bulky methyl

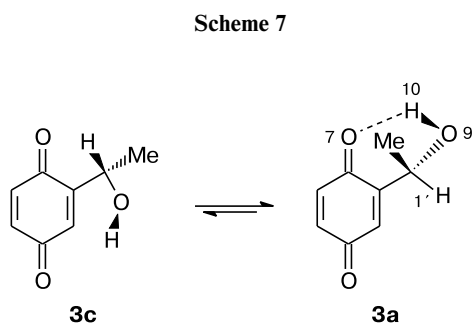
substituent near the C(1)O carbonyl group lying in the plane of the benzoquinone ring) and to the ability of the 1'-OH group to participate in the formation of the IMHB with the carbonyl group. Owing to the orientation effect of the latter, one-step interconversion $\mathbf{a} \rightleftharpoons \mathbf{b}$ occurs as concerted rotation of the 1'-OH group and the whole substituent about the C(1')-O(9) and C(1')-C(2) bonds. This basically distinguishes these transitions from the transitions between rotamers with the free 1'-OH group. For



instance, transitions $c \rightleftharpoons e$ and $e \rightleftharpoons d$ can occur as a result of rotation of the 1'-OH group only, while transitions $c \rightleftharpoons f$ can occur as a result of rotation of the substituent (in this case, $\theta_{OH} \approx \text{const}$). An exception is the transition $d \rightleftharpoons g$, which causes the θ_{OH} angle to change by about 20° .

Thus, molecule **3** can exist in the gas phase as a mixture of seven nonplanar rotamers **3a–g**. In two of them (**3a,b**) the 1'-OH group is involved in the formation of IMHB.

The Gibbs free energies ($G = E_0 + G_7$) were calculated using the default scheme implemented in the GAUSSIAN-03 program. B3LYP calculations in the 6-311G(d), 6-311G(d,p), cc-pVDZ, and cc-pVTZ basis sets predict the lowest G value for rotamer **3c** (see Table 1) with $R(O(7)-O(9)) = 4.213 \text{ \AA}$. The IMHB between the H atom of the 1'-OH group and the carbonyl O atom of benzoquinone is very weak; the inclusion of the entropy factor causes a shift of the equilibrium toward the rotamers with the free 1'-OH group. The strength of the IMHB was estimated as the enthalpy difference between rotamers **3c** and **3a** (Scheme 7): $\Delta H = H_{3a} - H_{3c} = -0.15 \text{ kcal mol}^{-1}$ (cf. $\Delta G = G_{3a} - G_{3c} = 0.20 \text{ kcal mol}^{-1}$).



The effect of solvent (cyclohexane) on the geometric parameters and energy characteristics of molecule **3** was modeled by the B3LYP method with the 6-311G(d) and

cc-pVTZ basis sets in the framework of the polarizable continuum model (PCM).²⁵ The thermal corrections, G_T , to the Gibbs free energy were calculated in the 6-311G(d) basis set.¹⁸ Rotamers **3f** and **3g** having percentages of at most 0.18 were left out of consideration. The stretching vibration frequencies calculated with inclusion of the solvent effect decrease by 4–8 cm^{-1} for rotamers **3a,b** and by 0–4 cm^{-1} for rotamers **3c–e** (see Table 1). In the gas phase, the ratio (Y) of the percentage of the rotamers with free OH groups to that of the rotamers with bound OH groups is 1.58 (B3LYP/6-311G(d)) and 1.89 (B3LYP/6-311G(d,p)). In cyclohexane, Y increases to 2.15 (B3LYP/6-311G(d)). More exact calculations of Y in the cc-pVTZ basis set give a value of 1.68 (gas phase) and 2.41 (cyclohexane). The ratio of the areas-under-curve, $S_{3635}/(S_{3586} + S_{3570})$, calculated from the experimental spectrum of compound **3** in hexane (cyclohexane) solution is 1.77. Assuming that the absolute intensities of the $\nu(\text{OH})$ bands of the free and bound OH groups differ insignificantly, good qualitative agreement with the "experimental" Y value is provided by the Y values estimated from the results of B3LYP/6-311G(d,p) and B3LYP/cc-pVTZ (gas phase) calculations. B3LYP/cc-pVTZ calculations with inclusion of the solvent effect in the framework of the PCM model overestimate the Y value. This is probably due to the assumption made above.

The estimates of the Y ratio were obtained using the results of calculations with no frequency scaling. When the frequencies are scaled with a factor of 0.95, the Y values change insignificantly, to 1.56 and 1.66 (cf. 1.58 and 1.68, respectively, with no scaling; B3LYP/6-311G(d) and B3LYP/cc-pVTZ calculations). The scale factor was chosen to be equal to the ratio of the frequency observed in the spectrum of compound **3** for free 1'-OH group (3635 cm^{-1}) to the average theoretically calculated frequency ($(3811.2 + 3805.1 + 3830.3)/3 = 3815.5 \text{ cm}^{-1}$).

Detailed conformational analysis of molecule **3** (see above) allows one to interpret the contour of the $\nu(\text{OH})$ band in the IR spectra of solutions of **3** in inert solvents. The larger splitting of this band ($\sim 50 \text{ cm}^{-1}$) is due to the equilibrium between the rotamers **3a,b** with the bound OH group and the rotamers **3c–g** with the free OH group. Each of the two components of the $\nu(\text{OH})$ band originates from the contributions of several rotamers. For instance, the smaller splitting (16 cm^{-1}) of the low-frequency component of the $\nu(\text{OH})$ band is due to the equilibrium $3a \rightleftharpoons 3b$. The difference $\nu(\text{OH})_{3b} - \nu(\text{OH})_{3a} = 13.5 \text{ cm}^{-1}$ calculated in the cc-pVTZ basis set for the gas phase is in reasonable agreement with the observed splitting (16 cm^{-1}) in the spectrum of a solution of compound **3** in hexane (see Fig. 4). Broadening of spectral bands in CCl_4 and, especially, chloroform makes the low-frequency component unresolvable, but, mathematically, the contour is described in this case by a doublet. According to gas-phase calculations in the cc-pVTZ basis set, the $\nu(\text{OH})$ frequen-

cies of rotamers **3c** and **3d** differ by 5 cm^{-1} only and thus are expected to appear in the spectra as a single band. The calculated $\nu(\text{OH})$ frequency of rotamer **3e** differs from those of rotamers **3c** and **3d** by about 17 cm^{-1} and would appear as a particular band with allowance for the percentage of **3e** (21.9%). However, in the spectrum of a solution of compound **3** in hexane (see Fig. 4) the band at 3635 cm^{-1} only has an asymmetric contour. This may indicate that the B3LYP/cc-pVTZ method overestimates the frequency of rotamer **3e**. Owing to very low content of the rotamers **3f** and **3g**, the contributions of their $\nu(\text{OH})$ to the bandshape can be neglected. Thus, calculations predict a high percentage of rotamers with the free OH group in both the gas phase and solution, which corresponds to the more intense high-frequency component band $\nu(\text{OH})$ in the spectrum of compound **3**.

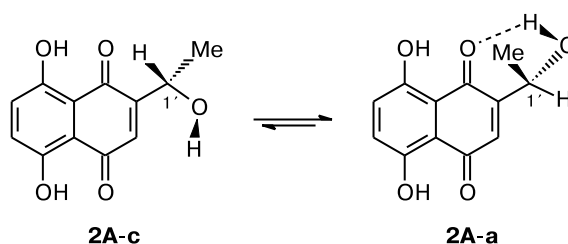
Next, we studied the conformational mobility of compound **2**. For all rotamers of **2**, the initial values of geometric parameters of the $1'\text{-OH}$ group in all four tautomeric forms were equal to those obtained upon geometry optimization of the model benzoquinone **3**. Prescreening of tautomeric-rotameric states of molecule **2** was performed in the 6-31G(d) basis set. Having estimated the percentage of all 28 tautomeric-rotameric states (seven rotamers for each out of four tautomers), we refined the geometric and energy characteristics of the isomers having percentages higher than 1% in more extended basis sets 6-311G(d), 6-311G(d,p), and cc-pVDZ. The results of calculations of the energy characteristics of all isomers of compound **2** are listed in Table 2. The structures of all rotamers for the tautomeric forms **2A** and **2B** are shown in Figs 2 and 3.

Conformational analysis of molecule **2** showed that the content of all rotamers in the tautomeric forms **A** and **B** is 100% (form **A** — 85.8%, form **B** — 14.2%; B3LYP/6-311(d) calculations); among them, the content of the rotamers with IMHB is only 35.6% (see Table 2). Therefore, the energy and geometric characteristics of isomers of compound **2** were then refined in the G-311G(d,p) and cc-pVDZ basis sets only for the tautomeric forms **A** and **B**.

Among all 28 isomers, the quinonoid isomer **2A-a** has the lowest energy E_0 . As for compound **3**, the inclusion of the entropy factor causes the equilibrium between the isomers (Scheme 8) to shift toward **2A-c** ($\Delta G = G_{2A-a} - G_{2A-c} = 0.13\text{ kcal mol}^{-1}$, see Table 2). The enthalpy difference $\Delta H = H_{2A-a} - H_{2A-c} = -0.10\text{ kcal mol}^{-1}$ (B3LYP/cc-pVDZ calculations).*

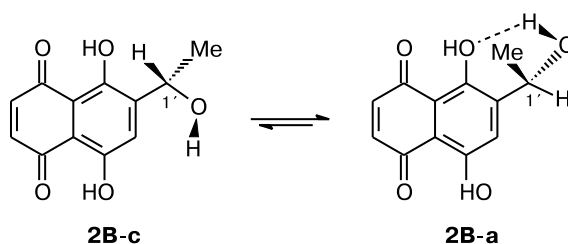
Among the benzenoid tautomers, isomer **2B-c** (Scheme 9) has the lowest energy E_0 . The inclusion of the entropy factor causes the equilibrium to shift toward rotamers with no IMHB to even greater extent, *viz.*, one gets $\Delta G = G_{2B-a} - G_{2B-c} = 0.63\text{ kcal mol}^{-1}$. In contrast to the

Scheme 8



model benzoquinone **3** and the quinonoid tautomers of compound **2**, the enthalpy difference $\Delta H = H_{2B-a} - H_{2B-c}$ is $0.39\text{ kcal mol}^{-1}$. Thus, the formation of IMHB in the benzenoid tautomers is an endothermic process.

Scheme 9



As mentioned above, isomers of only two tautomeric forms, **2A** and **2B**, dominate in the gas phase. For **2B**, the percentage of all rotamers is at most 16% (among them, only 4.4% of rotamers with IMHB, see Table 2). Therefore, the shape of the contour of the $\nu(\text{OH})$ bands in the spectrum of compound **2** is mainly determined by the rotamers of the quinonoid tautomer **2A**. As in the spectrum of benzoquinone **3**, the high-frequency band at 3635 cm^{-1} in the spectrum of a solution of compound **2** in hexane is stronger than three low-frequency bands at 3605 , 3589 , and 3570 cm^{-1} (see Fig. 1). It corresponds to isomers of the tautomers **2A** and **2B** with no IMHB, while the low-frequency band corresponds to the isomers with the $1'\text{-OH}$ group involved in the formation of IMHB with the carbonyl O(1) atom. The ratio of the area-under-curve for the high-frequency component of the $\nu(\text{OH})$ band to the sum of the areas-under-curve for the low-frequency components is $Y = 1.62$, which is close to theoretical estimate of the ratio of the percentage of all rotamers with the free $1'\text{-OH}$ group to the percentage of rotamers with IMHB equal to 1.81 (calculations in the cc-pVDZ basis set for the gas phase). As was shown taking the model compound **3** as an example, the inclusion of the solvent effect on the equilibrium between rotamers causes the ratio Y to increase; this also seems to be valid for compound **2**.

The high-frequency $\nu(\text{OH})$ band appears in the spectrum as a single band owing to close frequencies of the rotamers **2A-c**, **2A-d**, and **2A-e**. More "diffuse" contour of

* From this point on, by default we will discuss the energy characteristics calculated in the cc-pVDZ basis set.

Table 2. Electronic energies (E_0 /au), total energies ($(E = E_0 + ZPE)$ /au), the Gibbs free energies (G /au), enthalpies (ΔH /kcal mol⁻¹), relative Gibbs free energies (ΔG /kcal mol⁻¹), percentages ($g^{\%}$ (%)), $\nu(\text{OH})$ frequencies/cm⁻¹, and intensities A (rel. units) calculated for rotamers of 1'-hydroxyethyl-1,4-naphthazarine **2**

Rotamer	Computational method	$-E_0$	$-E$	$-G$	$-H$	ΔG	$g^{\%}$	ν/A
2A-a	B3LYP/6-31G(d)	839.420320	839.216262	839.256446	839.201427	0.00	36.32	3687.8/1.00
	B3LYP/6-311G(d)	839.623313	839.419706	839.459991	839.459991	0.24	20.16	3734.5/1.00
	B3LYP/6-311G(d,p)	839.653552	839.450465	839.490772	839.435544	0.27	19.81	3765.2/1.00
	B3LYP/cc-pVDZ	839.489155	839.286194	839.326344	839.271391	0.13	23.35	3700.4/1.00
2A-b	B3LYP/6-31G(d)	839.419496	839.215299	839.255404	839.200539	0.65	12.13	3697.6/1.04
	B3LYP/6-311G(d)	839.623123	839.419330	839.459512	839.404526	0.54	12.15	3746.4/1.10
	B3LYP/6-311G(d,p)	839.652992	839.449772	839.490003	839.434923	0.73	9.11	3776.6/1.09
	B3LYP/cc-pVDZ	839.488355	839.285246	839.325307	839.270552	0.78	7.79	3712.3/1.10
2A-c	B3LYP/6-31G(d)	839.419095	839.215516	839.255985	839.200473	0.29	22.26	3734.3/0.23
	B3LYP/6-311G(d)	839.622935	839.419773	839.460372	839.404678	0.00	30.23	3773.8/0.31
	B3LYP/6-311G(d,p)	839.653305	839.450620	839.491197	839.435506	0.00	31.25	3820.6/0.39
	B3LYP/cc-pVDZ	839.488848	839.286193	839.326547	839.271224	0.00	29.08	3767.3/0.22
2A-d	B3LYP/6-31G(d)	839.417926	839.214354	839.254742	839.199314	1.07	5.97	3729.1/0.26
	B3LYP/6-311G(d)	839.621411	839.418322	839.458865	839.403194	0.95	6.08	3768.2/0.36
	B3LYP/6-311G(d,p)	839.652097	839.449408	-839.489891	839.434298	0.82	7.83	3815.3/0.40
	B3LYP/cc-pVDZ	839.487774	839.285178	-839.325510	839.270200	0.65	9.71	3757.9/0.28
2A-e	B3LYP/6-31G(d)	839.418266	839.214835	839.255325	839.199731	0.70	11.14	3759.4/0.31
	B3LYP/6-311G(d)	839.622332	839.419299	839.459832	839.404168	0.34	17.03	3801.7/0.40
	B3LYP/6-311G(d,p)	839.652679	839.450147	839.490707	839.434978	0.31	18.52	3845.5/0.53
	B3LYP/cc-pVDZ	839.488079	839.285608	839.325978	839.270572	0.36	15.84	3791.7/0.38
2A-f	B3LYP/6-31G(d)	839.412663	839.209231	839.249863	839.194105	4.13	0.03	3736.0/0.18
	B3LYP/6-311G(d)	839.616144	839.413091	839.453786	839.397938	4.13	0.03	3775.7/0.25
2A-g	B3LYP/6-31G(d)	839.413526	839.209901	839.250814	839.194788	3.53	0.09	3717.7/0.14
	B3LYP/6-311G(d)	839.616945	839.413730	839.454735	839.398570	3.54	0.08	3755.0/0.19
2B-a	B3LYP/6-31G(d)	839.417847	839.214039	839.254138	839.199157	1.45	3.14	3716.1/0.57
	B3LYP/6-311G(d)	839.621145	839.417714	839.457896	839.402782	1.55	2.21	3754.8/0.67
	B3LYP/6-311G(d,p)	839.651228	839.448374	839.488578	839.433413	1.64	1.96	3790.5/0.65
	B3LYP/cc-pVDZ	839.486793	839.284120	839.324182	839.269278	1.48	3.50	3734.0/0.57
2B-b	B3LYP/6-31G(d)	839.416816	839.212847	839.252871	839.198052	2.24	0.83	3721.2/0.60
	B3LYP/6-311G(d)	839.620718	839.417086	839.457182	839.402153	2.00	1.03	3763.4/0.71
	B3LYP/6-311G(d,p)	839.650398	839.447406	839.487558	839.432521	2.28	0.67	3798.8/0.70
	B3LYP/cc-pVDZ	839.485705	839.282889	839.322886	839.268122	2.30	0.90	3742.0/0.64
2B-c	B3LYP/6-31G(d)	839.417680	839.214173	839.254599	839.199124	1.16	5.13	3733.9/0.22
	B3LYP/6-311G(d)	839.621616	839.418478	839.458990	839.403385	0.87	6.96	3773.7/0.30
	B3LYP/6-311G(d,p)	839.651828	839.449221	839.489740	839.434104	0.91	6.73	3820.3/0.38
	B3LYP/cc-pVDz	839.487424	839.284879	839.325186	839.269907	0.85	6.93	3767.0/0.27
2B-d	B3LYP/6-31G(d)	839.416180	839.212668	839.252950	839.197637	2.19	0.90	3730.1/0.26
	B3LYP/6-311G(d)	839.619772	839.416671	839.457092	839.401549	2.06	0.93	3769.3/0.37
	B3LYP/6-311G(d,p)	839.650272	839.447667	839.488032	839.432564	1.99	1.09	3816.5/0.41
	B3LYP/cc-pVDZ	839.486032	839.283548	839.323771	839.268577	1.74	1.54	3759.1/0.29
2B-e	B3LYP/6-31G(d)	839.416543	839.213224	839.253672	839.198106	1.74	1.93	3759.1/0.30
	B3LYP/6-311G(d)	839.620662	839.417722	839.458200	839.402577	1.36	3.04	3801.7/0.38
	B3LYP/6-311G(d,p)	839.650891	839.448486	839.488991	839.433304	1.38	3.04	3845.6/0.51
	B3LYP/cc-pVDZ	839.486366	839.284032	839.324335	839.268988	1.39	2.78	3791.9/0.37
2B-f	B3LYP/6-31G(d)	839.411744	839.208421	839.249004	839.193269	4.67	0.01	3737.0/0.17
	B3LYP/6-311G(d)	839.616078	839.412153	839.452842	839.396961	4.73	0.01	3776.4/0.24
2B-g	B3LYP/6-31G(d)	839.411943	839.208440	839.249299	839.193311	4.48	0.02	3719.6/0.14
	B3LYP/6-311G(d)	839.615334	839.412223	839.453208	839.397043	4.50	0.02	3757.3/0.18
2C-a	B3LYP/6-31G(d)	839.413445	839.210063	839.250037	839.195333	4.02	0.04	3667.1/1.19
	B3LYP/6-311G(d)	839.615778	839.412660	839.452709	839.397886	4.81	$9.0 \cdot 10^{-3}$	3715.2/1.32

(to be continued)

Table 2 (continued)

Rotamer	Computational method	$-E_0$	$-E$	$-G$	$-H$	ΔG	$g\%$	ν/A
2C-b	B3LYP/6-31G(d)	839.412489	839.209011	839.248930	839.194347	4.72	0.01	3676.3/1.23
	B3LYP/6-311G(d)	839.615481	839.412189	839.452141	839.397502	5.17	$5.0 \cdot 10^{-3}$	3727.1/1.30
2C-c	B3LYP/6-31G(d)	839.411773	839.208983	839.249306	839.194014	4.48	0.02	3734.0/0.23
	B3LYP/6-311G(d)	839.614979	839.412377	839.452800	839.452800	4.75	0.01	3773.5/0.31
2C-d	B3LYP/6-31G(d)	839.410542	839.207806	839.248071	839.192827	5.26	0.01	3730.1/0.28
	B3LYP/6-311G(d)	839.613396	839.410911	839.451306	839.395860	5.69	$2.0 \cdot 10^{-3}$	3769.8/0.38
2C-e	B3LYP/6-31G(d)	839.411069	839.208412	839.248730	839.193388	4.84	0.01	3759.9/0.32
	B3LYP/6-311G(d)	839.614526	839.412035	839.452363	839.397002	5.03	$6.0 \cdot 10^{-3}$	3802.0/0.40
2C-f	B3LYP/6-31G(d)	839.405094	839.202516	839.242997	839.187463	8.44	$2.3 \cdot 10^{-5}$	3735.6/0.17
	B3LYP/6-311G(d)	839.607879	839.405429	839.445934	839.390389	9.06	$6.9 \cdot 10^{-6}$	3775.1/0.25
2C-g	B3LYP/6-31G(d)	839.405689	839.202943	839.243877	839.187876	7.89	$6.0 \cdot 10^{-5}$	3718.8/0.14
	B3LYP/6-311G(d)	839.608422	839.405856	839.446852	839.390753	8.48	$1.8 \cdot 10^{-5}$	3756.7/0.19
2D-a	B3LYP/6-31G(d)	839.409988	839.207240	839.247264	839.192425	5.76	$2.0 \cdot 10^{-3}$	3721.5/0.59
	B3LYP/6-311G(d)	839.612562	839.409819	839.449884	839.394984	6.58	$4.5 \cdot 10^{-4}$	3761.1/0.67
2D-b	B3LYP/6-31G(d)	839.409086	839.206131	839.246076	839.191405	6.51	$6.1 \cdot 10^{-4}$	3727.5/0.64
	B3LYP/6-311G(d)	839.612251	839.409289	839.449278	839.394550	6.96	$2.4 \cdot 10^{-4}$	3770.5/0.76
2D-c	B3LYP/6-31G(d)	839.409952	839.207353	839.247641	839.192401	5.53	$3.0 \cdot 10^{-3}$	3733.8/0.24
	B3LYP/6-311G(d)	839.613160	839.410622	839.450976	839.395653	5.90	$1.0 \cdot 10^{-3}$	3772.9/0.33
2D-d	B3LYP/6-31G(d)	839.408614	839.206010	839.246178	839.191673	6.44	$6.9 \cdot 10^{-4}$	3729.6/0.28
	B3LYP/6-311G(d)	839.611435	839.408954	839.449213	839.393964	7.00	$2.2 \cdot 10^{-4}$	3768.1/0.38
2D-e	B3LYP/6-31G(d)	839.408805	839.206427	839.246748	839.191405	6.09	$1.0 \cdot 10^{-3}$	3759.6/0.33
	B3LYP/6-311G(d)	839.612183	839.409842	839.450159	839.394823	6.41	$6.1 \cdot 10^{-4}$	3801.3/0.41
2D-f	B3LYP/6-31G(d)	839.404403	839.201949	839.242400	839.186900	8.81	$1.3 \cdot 10^{-5}$	3736.5/0.19
	B3LYP/6-311G(d)	839.607082	839.404696	839.445187	839.389647	9.53	$3.1 \cdot 10^{-6}$	3776.0/0.27
2D-g	B3LYP/6-31G(d)	839.404701	839.201978	839.242557	839.186978	8.72	$1.5 \cdot 10^{-5}$	3718.2/0.15
	B3LYP/6-311G(d)	839.607413	839.404796	839.445413	839.389774	9.39	$4.0 \cdot 10^{-6}$	3756.0/0.20

this band is also favored by the overlap of the $\nu(\text{OH})$ bands of the rotamers **2B-c**, **2B-d**, and **2B-e** with close frequencies (their contribution is at most 12%). The splitting of the low-frequency component of the $\nu(\text{OH})$ band ($\sim 19 \text{ cm}^{-1}$) is in reasonable agreement with the frequency difference between the rotamers **2A-a** and **2A-b** calculated in the cc-pVDZ basis set (12 cm^{-1}).

A weak $\nu(\text{OH})$ band at 3605 cm^{-1} in the spectrum of a solution of compound **2** in hexane probably originates from the "benzenoid" tautomers **2B-a** and **2B-b** whose frequencies differ by only 8 cm^{-1} (see Table 2), as predicted by calculations in the 6-311G(d,p) and cc-pVDZ basis sets. Therefore, it is most likely that they will appear in the spectra as a single band. The frequency difference estimated from the results of calculations in the cc-pVDZ basis set, $\nu_{\text{OH}}(\mathbf{2A-a}) - \nu_{\text{OH}}(\mathbf{2B-a}, \mathbf{2B-b}) = (3734 + 3742)/2 - 3700 = 38 \text{ cm}^{-1}$, is in good agreement with the frequency difference between maxima of the $\nu(\text{OH})$ bands in the spectrum of compound **2**: $3605 - 3570 = 35 \text{ cm}^{-1}$ (see Fig. 1).

Two-dimensional sections of the PES of benzoquinone **3** in the plane of the $\theta_{\text{O}(9)}$ and θ_{OH} torsion angles were

obtained from B3LYP/6-31G calculations. Analysis of their topography revealed seven rotamers. In two of them, the $1'-\text{OH}$ group is involved in the IMHB with the carbonyl O(1) atom.

The global minimum on the Gibbs free energy surface $G_0(\vec{R})$ corresponds to rotamer **3c** with the free $1'-\text{OH}$ group. In the gas phase, the percentage of rotamers with the free $1'-\text{OH}$ group is about 63% (estimated from the Gibbs free energy values), which is in qualitative agreement with experimental data. With allowance for the solvent (cyclohexane) effect in the framework of the PCM model, this estimate increases to nearly 71%.

Thus, we carried out the conformational analysis of $1'$ -hydroxyethylnaphthazarine **2** in the 6-31G(d), 6-311G(d), 6-311G(d,p), and cc-pVDZ basis sets. As for compound **3**, four tautomeric forms are possible for naphthazarine **2** and seven rotamers are possible for each tautomer. The most abundant is tautomeric form **A** (percentage $\sim 86\%$) in which the substituent bearing the $1'-\text{OH}$ group is in the quinonoid nucleus. Rotamer **2A-c** with free $1'-\text{OH}$ group has the lowest Gibbs free energy. In the gas phase, the percentage of all rotamers with free $1'-\text{OH}$

group exceeds 60%, which is in qualitative agreement with the pattern of the $\nu(\text{OH})$ bands in the IR spectra of a solution of **2** in hexane. The larger splitting of the $\nu(\text{OH})$ band in the IR spectra of solutions of **2** in nonpolar solvents is due to different frequencies of the rotamers resulting from cleavage of the relatively weak IMHB between the 1'-OH group and the carbonyl group. The energy of the IMHB was estimated at $0.10 \text{ kcal mol}^{-1}$.

Experimental

Quantum chemical calculations were carried out in the framework of the density functional theory (exchange-correlation functional B3LYP²⁶) with the 6-31G(d), 6-311G(d), 6-311G(d,p), cc-pVDZ, and cc-pVTZ basis sets and the GAUSSIAN 03 program²⁷ (by-default algorithms were used). Geometric parameters were optimized in internal coordinates using the Berni algorithm ("Tight" mode). Integrals were calculated by numerical integration on a grid with by-default parameters.

In constructing the 2D section of the PES, the energies (E_0) of the ground electronic state of 1'-hydroxyethylbenzoquinone **3** were calculated by optimizing all geometric parameters of the molecule except for θ_{OH} and $\theta_{\text{O(9)}}$ (these angles were chosen as the PES scan variables). Stationary points on the PES were located upon full optimization of the molecular geometry.

Geometry optimization was conducted until meeting the following condition for the norm of the gradient: $|\text{grad}| \leq 10^{-6} \text{ au } \text{\AA}^{-1}$. If normal-mode vibrational frequency calculations at certain stationary points on the PES gave no imaginary frequencies, these stationary points were treated as energy minima.

The Gibbs free energies, G , were calculated with inclusion of all electronic, translational, rotational, and vibrational degrees of freedom for $T = 298.15 \text{ K}$. The expression used for a molecule in the gas phase is as follows: $G_i = E_{0,i} + G_{T,i}$, where i is the number of the rotamer and $G_{T,i} = G_{T,i,t} + G_{T,i,v} + G_{T,i,r}$ is the sum of the rotational, vibrational, and translational contributions, respectively, calculated in the "harmonic oscillator—rigid rotor" approximation. The Gibbs free energy of the i th rotamer of the molecule in solution (s) was calculated in the framework of the PCM model²⁵ as $G_{i,s} = (E_{0,i})_s + (G_{T,i})_s$, where $(E_{0,i})_s$ is the electronic contribution and $(G_{T,i})_s$ is the sum of the translational, vibrational, and rotational contributions calculated using the PC GAMESS program²⁸ with inclusion of electrostatic interaction between the molecule and the solvent. All calculations were performed for the optimized structures using the by-default algorithms. The molecular geometry was optimized with the quadratic approximation (QA) algorithm. Integrals were calculated with an accuracy of 11 decimal places, the norm of the gradient was minimized until a value of $10^{-6} \text{ Hartree Bohr}^{-1}$. The percentage of the i th rotamer was calculated as $g_i^{\%} = g_i \cdot 100\%$.

The melting points were determined on a Boetius apparatus and are uncorrected. ¹H and ¹³C NMR spectra were recorded on a Bruker Avance DRX-500 spectrometer (¹H, 500 MHz; ¹³C, 125 MHz) in CDCl₃ with Me₄Si as the internal reference. Mass spectra (EI) were recorded on an LKB-9000S instrument with direct inlet at electron ionizing energies of 18 and 70 eV. IR spectra were recorded on a Bruker Vector 22 Fourier spectrophotometer with a resolution of 2 cm^{-1} in solutions in *n*-hexane, cyclohexane, CCl₄, and CDCl₃ (CaF₂ cells, layer thickness 1.00

to 2.50 mm). The frequency and area-under-curve measurements and the decomposition of contours of the $\nu(\text{OH})$ stretching absorption bands were performed using the OPUS/IR 02 Version 3.0.2 program package. The reproducibility in frequency measurements was at least 0.5 cm^{-1} . The concentrations of solutions of the compounds under study were 5 to 20 mmol L⁻¹.

The course of reactions was monitored, and individual character of the compounds synthesized was confirmed, by TLC (Merck 60F-254 plates, hexane—acetone 3 : 1). Individual compounds were isolated from mixtures of reaction products by preparative TLC on 20×20-cm plates with fixed silica gel layer 5—40 μm thick. The yields of the compounds were not optimized. Elemental analysis was done on a Flash EA1112 C,H,N analyzer.

Acetylhydroquinone (6). To a melt of anhydrous AlCl₃ (145 g, 1.1 mol) and NaCl (27 g, 0.5 mol), hydroquinone diacetate (**4**) (31 g, 0.16 mol) was added portionwise with vigorous stirring at 140 °C. The temperature of the mixture was raised to 195 °C and the melt was stirred for 9 min. The reaction mixture was cooled and hydrolyzed with a solution of conc. HCl (150 mL) in water (2.0 L). After 12 h, the precipitate was filtered off, washed with hot water (0.5 L), and dried. A mixture of acetylhydroquinone *O*-acetate (**5**) and acetylhydroquinone (**6**) was obtained (26 g). ¹H NMR for **6** (δ , J/Hz): 2.60 (s, 3 H, Me); 4.62 (s, 1 H, C(4)OH); 6.89 (d, 1 H, H(6), $J = 8.5$); 7.03 (dd, 1 H, H(5), $J_1 = 8.5$, $J_2 = 2.9$); 7.19 (d, 1 H, H(3), $J = 2.9$); 11.81 (s, 1 H, C(1)OH). ¹H NMR for **5** (δ , J/Hz): 2.31, 2.62 (both s, 3 H, Me); 6.99 (d, 1 H, H(6), $J = 8.5$); 7.21 (dd, 1 H, H(5), $J_1 = 8.5$, $J_2 = 2.9$); 7.45 (d, 1 H, H(3), $J = 2.9$); 12.13 (s, 1 H, C(1)OH). A mixture of **5** and **6** was boiled for 0.5 h in HCl (100 mL), filtered, the residue was washed with water and dried to give 20.5 g (85%) of acetylhydroquinone (**6**), m.p. 198—200 °C (cf. Ref. 29: m.p. 202—203 °C). IR spectrum (CHCl₃), ν/cm^{-1} : 3601, 3100 (O—H); 1647 (C=O); 1629, ~1615, ~1600, 1590 (C=C). Mass spectrum, m/z (I_{rel} (%)): 153 [M + 1] (9.1), 152 [M]⁺ (100), 43 (2.9).

1'-Hydroxyethylbenzoquinone (3). Acetylhydroquinone **6** (150 mg, 1 mmol) was dissolved in PrⁱOH (10 mL) and sodium borohydride (40 mg, 1 mmol) was added with stirring. The course of the reaction was monitored by TLC (hexane—acetone, 3 : 1). A few minutes after completion of the reaction, the reaction mixture was diluted with water, carefully acidified with HCl until a weak acid reaction, and extracted with ethyl acetate. The extract was dried with Na₂SO₄, concentrated under reduced pressure, and the dark oily residue was dissolved in MeCN (3 mL). To this solution, a solution of 1 g (NH₄)₂Ce(NO₃)₆ in a mixture of MeCN (1 mL) and water (3 mL) was added dropwise with stirring and ice-cooling. The course of the reaction was monitored by TLC. After 30 min, the reaction mixture was poured onto ice and after an additional 1 h extracted with Et₂O. The ethereal layer was washed with water, dried with Na₂SO₄, and concentrated. The yield of 1'-hydroxyethylbenzoquinone (**3**) was 98 mg (65%), light-yellow oil; after additional purification by preparative TLC the oil crystallizes in a refrigerator, m.p. 55—57 °C. Found (%): C, 63.23; H, 5.28. C₈H₈O₃. Calculated (%): C, 63.15; H, 5.30. ¹H NMR (δ , J/Hz): 1.38 (d, 3 H, Me, $J = 6.5 \text{ Hz}$); 4.82 (qd, 1 H, CH, $J = 6.5$, $J = 1.4 \text{ Hz}$); 4.09 (br. s, 1 H, OH); 6.71 (m, 2 H, H(5), H(6)); 6.77 (q, 1 H, H(3), $J = 1.4 \text{ Hz}$). ¹³C NMR (δ): 188.0, 187.6 (C=O), 151.1 (C(2)), 136.9, 136.4 (C(5), C(6)), 130.5 (C(3)), 64.5 (C(1')), 22.6 (Me). Mass spectrum, m/z (I_{rel} (%)): 152 [M]⁺ (100), 136 (53), 135 (31), 123 (46), 109 (28), 95 (8), 76 (15).

References

1. R. Majima, C. Kuroda, *Acta Phytochim.*, 1922, **1**, 43.
2. H. Brockmann, *Justus Liebig's Ann. Chem.*, 1936, **521**, 1.
3. R. H. Thomson, *Naturally Occurring Quinones*, 2nd ed., Academic Press, London—New York, 1971, 734 p.
4. R. H. Thomson, *Naturally Occurring Quinones*, 3rd ed., Chapman Hall, London—New York, 1987, 732 p.
5. V. P. Papageorgion, *Planta Med.*, 1980, **38**, 193.
6. G. Hondos, F. Sakabibara, K. J. Yazaki, *J. Nat. Prod.*, 1988, **51**, 152.
7. M. Hayashi, *Nippon Yakurigaka Zasshi*, 1977, **73**, 193.
8. S. Tanaka, M. Tajima, M. Tsukada, M. Tabata, *J. Nat. Prod.*, 1986, **49**, 466.
9. B. Z. Ahn, K. U. Baik, G. R. Kweon, K. Lim, B. D. Hwang, *J. Med. Chem.*, 1995, **38**, 1044.
10. M. Hayashi, *Nippon Yakurigaka Zasshi*, 1977, **73**, 205.
11. M. Hayashi, *Nippon Yakurigaka Zasshi*, 1977, **73**, 177.
12. H. Wagner, B. Kreher, V. Jurcic, *Arznaim. Forsch.*, 1988, **38**, 273.
13. V. P. Papageorgiou, *Planta Med.*, 1979, **37**, 185.
14. U. Sanakawa, H. Otsuka, U. Kataoka, A. Iitaka, A. Hosi, K. Kuretani, *Chem. Pharm. Bull.*, 1981, **29**, 116.
15. K. Inoue, M. Akaji, H. Inouye, *Chem. Pharm. Bull.*, 1985, **33**, 3993.
16. V. P. Glazunov, N. D. Pokhilo, N. V. Bochinskaya, A. Ya. Yakubovskaya, V. F. Anufriev, *Izv. Akad. Nauk, Ser. Khim.*, 2003, 1544 [*Russ. Chem. Bull., Int. Ed.*, 2003, **52**, 1629].
17. M. Oki, H. Iwamura, *Bull. Chem. Soc. Jpn*, 1960, **33**, 681.
18. D. V. Berdyshev, V. P. Glazunov, V. L. Novikov, *Izv. Akad. Nauk, Ser. Khim.*, 2008, 499 [*Russ. Chem. Bull., Int. Ed.*, 2008, **57**, 510].
19. M. Z. Tabrizi, S. F. Tayyari, F. Tayyari, M. Behforouz, *Spectrochim. Acta, Part A*, 2004, **60**, 111.
20. Y. H. Mariam, L. Chantranupong, *J. Mol. Struct. (THEOCHEM)*, 2000, **529**, 83.
21. J. Ireta, J. Neugebauer, M. Scheffler, *J. Phys. Chem. A*, 2004, **108**, 5692.
22. J. R. Juhasz, L. F. Pisterzi, D. M. Gasparo, D. R. P. Almeida, I. G. Csizmadia, *J. Mol. Struct. (THEOCHEM)*, 2003, **666–667**, 401.
23. Y. H. Mariam, R. N. Musin, *J. Phys. Chem. A*, 2008, **112**, 134.
24. D. V. Berdyshev, V. P. Glazunov, V. L. Novikov, *Issledovaniya v oblasti fiziko-khimicheskoi biologii i biotekhnologii. Tez. dokl. regional'noi konf. [Research on Physicochemical Biology and Biotechnology. Abstrs Region. Conf.]*, Vladivostok, 2004, 24 (in Russian).
25. S. Miertus, E. Scrocco, J. Tomasi, *Chem. Phys.*, 1993, **55**, 117.
26. P. J. Stephens, F. J. Devlin, C. F. Chabalowski, M. J. Frisch, *J. Phys. Chem.*, 1994, **98**, 11623.
27. M. J. Frisch, G. W. Trucks, H. B. Schlegel, G. E. Scuseria, M. A. Robb, J. R. Cheeseman, J. A. Montgomery, Jr., T. Vreven, K. N. Kudin, J. C. Burant, J. M. Millam, S. S. Iyengar, J. Tomasi, V. Barone, B. Mennucci, M. Cossi, G. Scalmani, N. Rega, G. A. Petersson, H. Nakatsuji, M. Hada, M. Ehara, K. Toyota, R. Fukuda, J. Hasegawa, M. Ishida, T. Nakajima, Y. Honda, O. Kitao, H. Nakai, M. Klene, X. Li, J. E. Knox, H. P. Hratchian, J. B. Cross, V. Bakken, C. Adamo, J. Jaramillo, R. Gomperts, R. E. Stratmann, O. Yazyev, A. J. Austin, R. Cammi, C. Pomelli, J. W. Ochterski, P. Y. Ayala, K. Morokuma, G. A. Voth, P. Salvador, J. J. Dannenberg, V. G. Zakrzewski, S. Dapprich, A. D. Daniels, M. C. Strain, O. Farkas, D. K. Malick, A. D. Rabuck, K. Raghavachari, J. B. Foresman, J. V. Ortiz, Q. Cui, A. G. Baboul, S. Clifford, J. Cioslowski, B. B. Stefanov, G. Liu, A. Liashenko, P. Piskorz, I. Komaromi, R. L. Martin, D. J. Fox, T. Keith, M. A. Al-Laham, C. Y. Peng, A. Nanayakkara, M. Challacombe, P. M. W. Gill, B. Johnson, W. Chen, M. W. Wong, C. Gonzalez, J. A. Pople, *GAUSSIAN-03, Revision D.01*, Gaussian, Inc., Wallingford (CT), 2004.
28. A. V. Nemukhin, B. L. Grigorenko, A. A. Granovskii, *Vestn. MGU, Ser. 2. Khimiya*, 2004, **45**, 75 [*Vestn. Mosk. Univ., Ser. Khim. (Engl. Transl.)*, 2004, **45**].
29. *Dictionary of Organic Compounds*, Ed. J. Buckingham, 5th ed., Chapman Hall, New York—London—Toronto, 1982.

Received March 12, 2008;
in revised form June 11, 2008